Transactions of the Materials Research Society of Japan 25 [4] 933-938 (2000)

Excitonic Properties of Silicon Nanoparticles: A Model Material for Molecular Electronics

Yoshihiko Kanemitsu
Graduate School of Materials Science, Nara Institute of Science and Technology, Ikoma, Nara 630-0101, Japan
Fax: 81-743-72-6011, e-mail: sunyu@ms.aist-nara.ac.jp

We have summarized photoluminescence (PL) properties of crystalline silicon (c-Si) and amorphous silicon (a-Si) based nanostructures and discuss the quantum confinement and spatial localization of excitons and carriers in silicon quantum materials. The PL peak energies of c-Si and a-Si quantum dots and wells are blueshifted from those of bulk c-Si and a-Si. Resonantly excited PL and time-resolved PL spectra show that both excitons confined in the Si well and excitons localized at the Si-SiO_2 interface determine PL properties in Si/SiO_2 quantum dots and wells. The understanding of quantum confinement and spatial localization of excitons and carriers is important for the development of molecular electronics devices.
Key words: silicon, quantum materials, nanocrystal, exciton, quantum confinement, localization

1. INTRODUCTION

Crystalline silicon (c-Si) is the dominant material in modern microelectronics. c-Si does not show efficient light emission at room temperature, because of its band structure with an indirect gap of 1.1 eV. Recently, efficient visible photoluminescence (PL) in porous c-Si and Si nanocrystals has been reported and new opto-electronic devices based on light-emitting Si nanostructures have been proposed [1-3]. Since the discovery of visible luminescence from porous c-Si [4], Si nanocrystals [5], Ge nanocrystals [6], and porous SiC [7], there are many extensive studies concerning the origin of visible light emission in c-Si and indirect-gap semiconductor nanoparticles. However, the mechanism of visible luminescence from c-Si nanoparticles is still controversial.

Well-controlled Si nanostructures are desired for the understanding the origin of visible PL from Si nanoparticles [8,9]. Si quantum dots (QD) and wells (QW) with SiO_2 surface layers have some advantages because SiO_2 is a well-characterized material known to passivate Si surface where Si/SiO_2 system is fully compatible with Si technology [10]. In this paper, we summarize our recent spectroscopic studies on Si/SiO_2 QD and QW structures and discuss confinement and localization of excitons and carriers in low-dimensional Si quantum structures.

2. Si NANOPARTICLE: A NEW MATERIAL PHASE

Silicon is an element semiconductor, and is not compound semiconductor. Elemental silicon is a good material for the fabrication of very small structures, because there is no composition fluctuation in the nanoparticle interior state. In addition, we can prepare many different Si materials: small Si molecules, Si clusters, chain-like Si polymers, ladder Si polymers, planar siloxene, Si nanoparticles, amorphous silicon (a-Si), and so on [1]. Using these unique Si materials, we study the size and dimensionality dependence of optical responses of Si materials [11].

From the fundamental physics viewpoints, semiconductor nanocrystals or nanoparticles are unique materials, as illustrated in Fig. 1. When the nanocrystal size is smaller than the exciton Bohr radius in bulk, we can observe size-dependent optical properties. By changing the size of nanoparticles, we can control the delocalization volume of excitons and carriers. Nanoparticles are intermediate materials between small molecular clusters and bulk. In addition, nanocrystals are intermediate materials between the single crystals and amorphous limits. The quantum confinement effect on the electron wavefunctions in disordered materials is also interesting phenomena [12,13].

In nanocrystals, the quantum confinement effect plays an essential role in optical transitions. The band gap energy increases with a decrease of the nanocrystal size. Nanocrystals have large surface-to-volume ratios. The luminescence properties will depend on the size and surface structure of nanocrystals. Si nanocrystals show visible luminescence at room temperature and their luminescence properties are sensitive to the size and surface structure [1]. The optical properties of silicon nanocrystals are completely different from those of bulk silicon (indirect-gap semiconductor). The relaxation of the k selection

rule due to quantum confinement will be important role in the visible luminescence process in Si nanoparticles and nanostructures. Since the well-controlled Si nanostructures can be fabricated by modern sample preparation techniques, Si nanoparticles and small nanostructures are key materials for quantum physics and device applications of low-dimensional structures and for future molecular electronics.

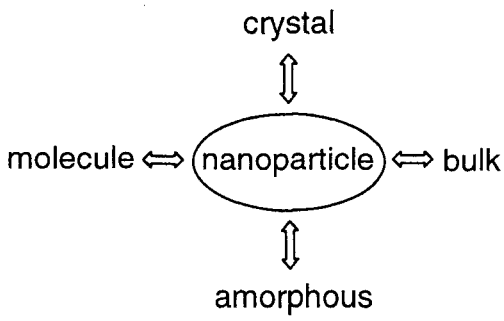

Figure 1. Si nanoparticles are unique materials. Nanoparticles are intermediate materials between small molecular clusters and bulk, and between the single crystal and amorphous limits.

The surface effect is important in Si nanocrystals optics. This is because silicon is one of elemental and nonpolar semiconductors. When Si nanocrystal is cover by SiO_2, the polar bonds are formed at the interface. These polar bonds such as Si-O, Si-OH, and Si=O will affect electronic properties of nonpolar interior state in very small dimensions [14,15]. On the other hand, hydrogen termination is a good passivation and reduces the surface states. It is believed that optical properties of surface-oxidized nanocrystals are completely different from those of H-terminated nanocrystals [9]. In order to clarify the surface effect, we prepared 0D nanocrystals and 2D wells and control the interior structure (a-Si or c-Si) and the surface structure (SiO_2 or SiH_2). These materials will be key materials for future Si nanodevices. Since Si/SiO_2 system is compatible with current Si technology, we discuss confinement and localization of excitons and carriers in Si/SiO_2 nanostructures.

3. NANOPARTICLES

c-Si and a-Si nanoparticles (QD) were prepared by an electrochemical anodization technique [16,17]. The electrochemical anodization of c-Si wafers and a-Si:H films was carried out in HF-ethanol solution ($HF:H_2O:C_2H_5OH=1:1:2$) at a constant current density of 10 mA/cm^2. Typical average sizes of c-Si and a-Si nanoparticles were 3 ~5 nm.

Figure 2 shows global PL spectra (non-resonantly excited PL spectra) of (a) bulk undoped a-Si, (b) a-Si QD, and (c) c-Si QD samples in the visible and near-infrared spectral region at 13 K. Bulk c-Si shows a sharp PL near 1.1 eV due to the TO-phonon-assisted optical transition. Undoped a-Si films show a broad PL near 1.4 eV. The a-Si and c-Si QD structures show visible PL. The size reduction to a few nanometers and the formation of nanoparticles cause the enhancement and blueshift of the band edge emission of a-Si:H (~1.4 eV) and c-Si (~1.1 eV) [18].

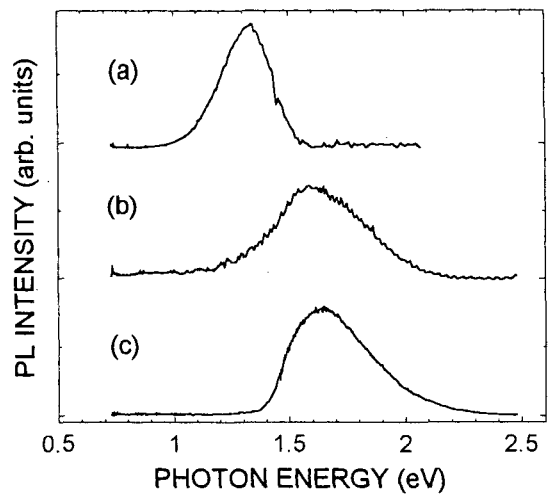

Figure 2. Global PL spectra of (a) bulk undoped a-Si, (b) a-Si QD, and (c) c-Si QD samples in the visible and near-infrared spectral region at 13 K.

The a-Si QD samples were fabricated by electrochemical etching of 1-% B-doped a-Si:H films. This starting material does not emit light in the 350-1700 nm spectral region. By forming nanoparticles from heavily doped a-Si:H films, the samples show luminescence near 1.6 eV. It is known that the luminescence efficiency of bulk a-Si:H depends on doping amount of acceptors or donors. Radiative recombination occurs at tail states near the band edge and non-radiative recombination occurs at midgap states. Heavily doped a-Si:H is a poor luminescent material even at low temperatures, because midgap states due to

defects are formed by doping. However, our experiments show that a-Si nanoparticles fabricated form heavily doped a-Si show efficient luminescence [18]. By fabricating nanostructures, the midgap states acting as nonradiative recombination centers would decrease. This is related to the formation of porous layer. The electrochemical etching of Si skeleton occurs preferentially at defects [19], and it is considered that a-Si nanoparticles in the porous layer (rest material) behave as undoped a-Si:H, a good luminescent material.

The observed PL spectrum of the a-Si QD sample is similar to that of the c-Si QD sample, as shown in Fig. 2. Under blue or green light excitation, c-Si and a-Si QD samples show broad luminescence even at low temperatures. These broad luminescence spectra are caused by contributions from all nanoparticles in the sample, because it is not easy to control the size distribution exactly in very small nanocrystals. The nanocrystal sample has a size fluctuation. Since the energy level in nanocrystals is determined by the nanocrystal size, the small nanocrystals show "blue" luminescence and the large nanocrystals show "red" luminescence. Therefore, we can selectively excite a subset of nanocrystals with a certain size in the sample by changing laser wavelength. For example, the long wavelength laser excites the large size crystals. As in many inhomogeneously broadened systems, selective excitation results in fluorescence line narrowing in nanocrystal samples. Selective excitation spectroscopy is one of powerful methods to obtain intrinsic information from inhomogeneously broaden spectra [20-24]. We applied selective excitation spectroscopy to naturally oxidized a-Si and c-Si QD samples.

Under resonant excitation at energies within the broad PL band, a-Si and c-Si samples show fine structures at low temperatures [23]. Under resonant excitation at the low-energy side of the PL band, phonon related structures are observed in a-Si and c-Si QD samples. In c-Si QD samples, the onset energy of the fine structures is equal to the TO (Δ) phonon energy of bulk c-Si. The observed peak energy in a-Si QD samples is equal to the TO phonon energy in bulk a-Si:H. The observed phonon structures in resonantly excited PL spectra show that the interior state of QD plays a dominant role in the PL process in large size nanoparticles [8,9,22,23].

On the other hand, under excitation at the high-energy side of the PL band, the Si-O-Si vibration structures appear in resonantly excited PL spectra of a-Si and c-Si QD samples, as summarized in Fig. 3. [16,18]. Since the Si-O bond is polar, the coupling of excitons and stretching vibrations of surface species increases with localization of excitons in smaller dimensions. The peak structures suggest that the localization of excitons at the Si/SiO_2 interface plays an essential role in the radiative recombination process in small nanoparticles [10,16].

Oxide termination may have several effects including the formation of interface states between c-Si and SiO_2 layer and a modification of the electronic structure of the c-Si interior state. In particular, when the size of nanocrystals is smaller than the bulk exciton Bohr radius, oxygen atoms at the interface induce the localization of excitons near the interface between c-Si and SiO_2, through the σ -n mixing and dipole interactions [8,25]. Both the disordered potential and the electronic interactions at the interface (Si=O or Si-OH bonds) induce exciton localization and then cause the size-insensitive PL spectrum in surface-oxidized Si nanocrystals [9,22].

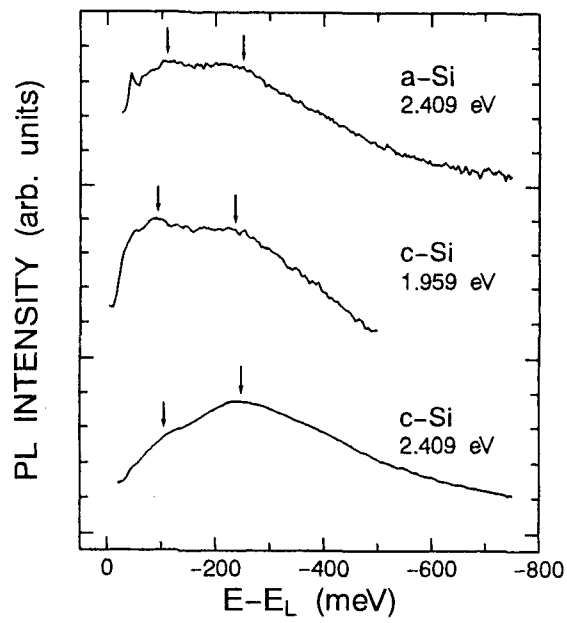

Figure 3. Resonantly excited PL spectra of a-Si and c-Si QD structures. Under resonant excitation at the high-energy side of the PL band, the Si-O-Si vibration structures indicated by the arrows appear in resonantly excited PL spectra. The excitation laser energies are shown in the figure.

Let now consider why a-Si QD samples show efficient luminescence and their PL peak energies are blueshifted from the PL peak energy of bulk a-Si. In a-Si, the localization length of carriers is

estimated to be about 0.6-1 nm [17,26-28]. No quantum confinement effects on the PL energy are expected for thickness larger than this critical length. However, the blueshift of the PL energy in 3-5 nm a-Si nanoparticles is clearly observed, as shown in Fig. 2. In addition, the PL energy in a-Si QW structures is blueshifted with a decrease of the a-Si well thickness, as will be discussed in the following section. These observations cannot be explained by the simple quantum confinement of carriers. We believe that the long-range carrier diffusion to non-radiative recombination centers does not occur in nanoparticles and very thin QW structures [29,30]. It is considered that that the carrier dynamics in a-Si QD structures are completely different from that in bulk a-Si. Figure 4 shows PL decay curves in a-Si and c-Si QD structures in the nanosecond time range at 10 K. The initial PL decay of a-Si QD structures is faster than that in c-Si QD structures [29]. The short lifetime in a-Si structures prevent the carrier relaxation into the deep states or long-range carrier diffusion to the nonradiative recombination centers. The short carrier lifetime is important in the observation of the blueshift of the PL spectrum in disordered a-Si materials [29,30].

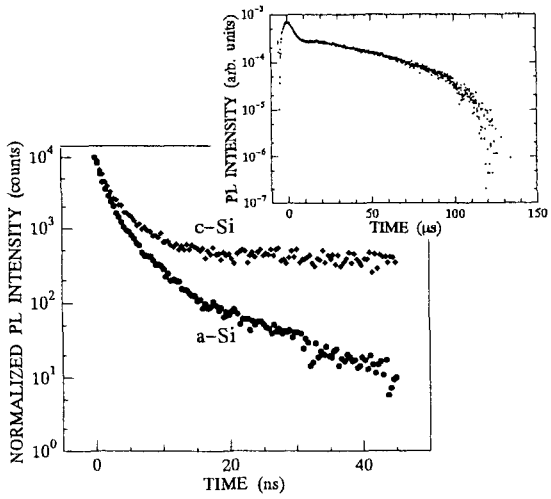

Figure 4. Initial PL decay profiles of a-Si and c-Si QD samples at 10 K. The inset shows a global PL decay curve in a c-Si QD sample at room temperature.

4. QUANTUM WELLS

In 0D Si nanoparticles, excitons are confined in three directions. In 2D Si wells, excitons are confined in one direction and can move in the 2D plane. The 2D wells are a weak confinement system, compared with the case of 0D nanoparticles. The comparison between 0D and 2D structures provides information on the ongoing discussion in quantum confinement and spatial localization of carriers and excitons in a-Si and c-Si quantum materials. The 2D QW structure have some advantages, because the well thickness is more exactly controlled in 2D systems, compared to the case of the 0D system.

Si single quantum well (QW) structures were formed on SIMOX (separation by implanted oxygen) wafers [31,32]. The 2D thin Si layers were formed between thin surface SiO_2 ($\sim$30 nm) and thick buried SiO_2 layers ($\sim$400 nm). Good crystalline quality in the Si layers was confirmed by the lattice image of high-resolution transmission electron microscopy and the reflectivity measurement.

a-Si/SiO_2 QW structures were formed by an e-beam deposition technique [30,33]. The SiO_2 layer thickness was 3.0 nm and the a-Si layer thickness was varied from 0.8 to 2.0 nm. The formation of thin Si layers was confirmed by high-resolution transmission electron microscopy (TEM) and x-ray reflectivity measurements.

Efficient PL in the visible spectral region was observed in very thin well samples ($<$2 nm) [30,32]. The inset of Fig. 5 shows PL spectra of 0.8-nm a-Si/SiO_2 and 0.8-nm c-Si/SiO_2 QW structures. The PL spectra of a-Si/SiO_2 and c-Si/SiO_2 QW structures depend on the a-Si and c-Si well thickness. The PL bandwidth in a-Si/SiO_2 QW structures is larger than that in c-Si/SiO_2 QW structures.

In the c-Si/SiO_2 QW structures, the asymmetric PL spectra in the red and infrared spectral region can be fitted by two Gaussian bands, the weak PL band and the strong PL band [32,34]. The peak energy of the strong band is almost independent of the well thickness and appears at $\sim$1.65 eV, as shown in the inset of Fig. 5. Therefore, the global PL spectrum in the c-Si/SiO_2 QW structure is not sensitive to the c-Si well thickness. In contrast, the peak energy of the weak band depends on the thickness of the c-Si well, and shifts to higher energy with a decrease of the Si well thickness. The size-dependent PL comes from optically anisotropic 2D quantum wells [32].

The thickness-dependent PL peak energies in c-Si/SiO_2 and a-Si/SiO_2 QW structures are summarized in Fig. 5. The PL peak energies in a-Si/SiO_2 QW structures are higher than those in c-Si/SiO_2 QW structures, because the PL energy in bulk a-Si is higher than that in bulk c-Si. With a decrease of the well thickness, the PL peak energy

is blueshifted in both a-Si/SiO_2 and c-Si/SiO_2 QW structures. The well-thickness dependence of the PL peak energy implies that quantum confinement effects play an essential role in luminescence processes in both c-Si/SiO_2 and a-Si/SiO_2 QW structures. However, the observed thickness-dependence of the PL energy in both c-Si/SiO_2 and a-Si/SiO_2 QW structures cannot be explained by simple quantum confinement models [25,35,36] and these dependence are different from the case of in a-Si/Si_3N_4 QW structures [37]. The exciton localization at the interface between the Si well layer and the SiO_2 barrier layer is also important in the radiative and nonradiative recombination processes [30].

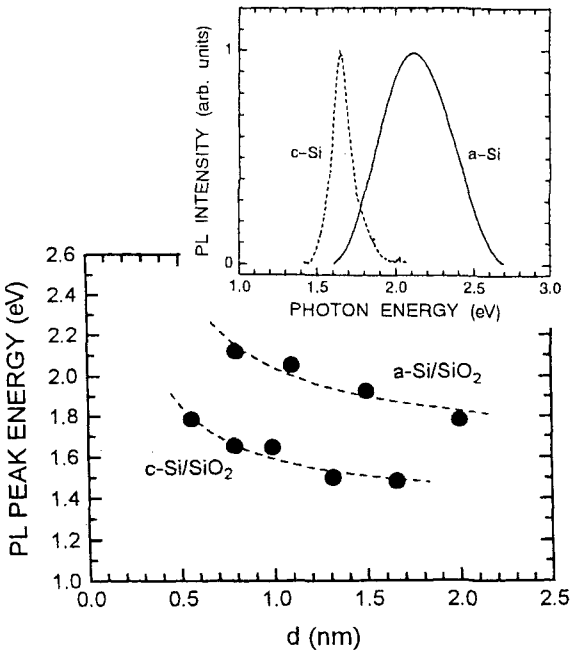

Figure 5. Well-thickness dependence of the PL peak energy in a-Si/SiO_2 and c-Si/SiO_2 QW structures. The inset is the PL spectra of 0.8-nm a-Si/SiO_2 and 0.8-nm c-Si/SiO_2 QW structures.

Let us consider why a pronounced blueshift is observed even in a-Si/SiO_2 QW structures. We measured PL lifetime in a-Si/SiO_2 QW structures at 10 K. In the red spectral region, the PL lifetime increases with a decrease of the PL photon energy and with an increase of the a-Si layer thickness. For example, in the 1.1-nm sample, the PL lifetimes at 2.4, 2.0, and 1.7 eV are 4, 20, and 80 ns, respectively [13]. The observed PL lifetime in a-Si/SiO_2 QW structures is shorter than the PL lifetime in bulk a-Si:H and the theoretically calculated radiative recombination lifetime in a-Si QW structures [38]. The PL dynamics behaviors of a-Si QW structures are similar to those of a-Si QD structures, as discussed in the previous section. In a-Si/SiO_2 QD and QW structures, the short lifetime of carriers reduces the energy relaxation of carriers into lower energy states and then increases the average energy of carriers in the band tail state [13]. Therefore, we can observe the pronounced blueshift of the PL peak energy in a-Si/SiO_2 QW and QD structures, because of the quantum confinement of carriers and the short carrier lifetime in a-Si interior states.

5. CONCLUSION

We have studied PL spectrum and dynamics of c-Si and a-Si based nanoparticles and 2D quantum wells and have discussed the nature of confinement and localization of excitons in Si quantum structures.

In large nanoparticles, luminescence is due to quantum-confined excitons in the interior state, while in small nanoparticles excitons are localized at the interface between Si and SiO_2. In 0D and 2D Si/SiO_2 systems, both excitons confined in the Si well and excitons localized at the Si-SiO_2 interface determine PL properties. In nonpolar semiconductor nanostructures, the polar surface bonds at the interface play an active role in luminescence processes in nanometer dimensions.

In a-Si/SiO_2 QD and QW structures, the short lifetime of carriers reduces the energy relaxation of carriers into lower energy states and then increases the average energy of carriers in the band tail state. It is concluded that the pronounced blueshift of the PL peak energy in a-Si/SiO_2 QW and QD structures is caused by the quantum confinement and localization of carries and the short carrier lifetime in a-Si interior states.

In this invited paper, we summarized our spectroscopic data on a-Si and c-Si based quantum structures. The detailed data have been published or will be published in journals. However, this comprehensive discussion on carrier localization and quantum confinement of carriers provides new insight of the luminescence mechanism and electronic structures of Si quantum materials.

ACKNOWLEDGEMENTS

The author would like to thank T. Kushida, J. N. Chazalviel, K. Nishimoto, Y. Takahashi, H. Kageshima, M. Iiboshi, Y. Fukunishi, and S. Okamoto for support and discussions. This work

was in part supported by a Grant-in-Aid for Scientific Research on Priority Areas (A) from the Ministry of Education, Science, Sports, and Culture of Japan (#11120231), a Grant-in-Aid for Scientific Research (B) from Japan Society for the Promotion of Science (# 11440095), The Yamada Science Foundation, and The Kawasaki Steel 21st Century Foundation.

REFERENCES

1. Y. Kanemitsu, Phys. Rep. **263**, 1 (1995).
2. A. G. Cullis, L. T. Canham, and P. D. J. Calcott, J. Appl. Phys. **82,** 909 (1997).
3. *Light Emission in Silicon*, Semiconductors and Semimetals vol. 49, edited by D. J. Lockwood (Academic, New York, 1997).
4. L. T. Canham, Appl. Phys. Lett. **57**, 1046 (1990).
5. H. Takagi, H. Ogawa, Y. Yamazaki, A. Ishizaki, and T. Nakagiri, Appl. Phys. Lett. **56**, 2346 (1990).
6. Y. Kanemitsu, H. Uto, Y. Masumoto, and Y. Maeda, Appl. Phys. Lett. **61**, 2187 (1991); Y. Maeda, N. Tsukamoto, Y. Yazawa, Y. Kanemitsu, and Y. Masumoto, Appl. Phys. Lett. **59**, 3168 (1991).
7. T. Matsumoto, J. Takahashi, T. Tamaki, T. Futagi, H. Mimura, and Y. Kanemitsu, Appl. Phys. Lett. **64**, 226 (1994); H. Mimura, T. Matsumoto, and Y. Kanemitsu, Appl. Phys. Lett. **65**, 3350 (1994).
8. Y. Kanemitsu, T. Ogawa, K. Shiraishi, and K. Takeda, Phys. Rev. B **48**, 4883 (1993).
9. Y. Kanemitsu and S. Okamoto, Mater. Sci. and Eng. B **48**, 108 (1997).
10. Y. Kanemitsu, N. Shimizu, T. Komoda, P. L. F. Hemment, and B. J. Sealy, Phys. Rev. B **54**, R14329 (1996).
11. Y. Kanemitsu, J. Lumin. **70**, 333 (1996).
12. Y. Kanemitsu, J. Lumin. **83/84**, 283 (1996).
13. Y. Kanemitsu, M. Iiboshi and T. Kushida, submitted for publication.
14. H. Kageshima and K. Shiraishi, Mater. Res. Soc. Proc. **486** (1997) 337.
15. H. Kageshima and K. Shiraishi, Surf. Sci. **380**, 61 (1997).
16. Y. Kanemitsu and S. Okamoto, Phys. Rev. B **56**, R1696 (1997).
17. R. B. Wehrsphonh, J.-N Chazalviel, F. Ozanam, and I. Solomon, Eur. Phys. J. B **8** (1999) 179.
18. Y. Kanemitsu, Y. Fukunishi, and T. Kushida, submitted for publication.
19. R. Schmuki, L. E. Erickson, and D. J. Lockwood,, Phys. Rev. Lett. **80**, 4060 (1998).
20. P. D. J. Calcott, K. J. Nash, L. T. Canham, M. J. Kane, and D. Brumhead, J. Phys. Condens. Matter. **5**, L91 (1993).
21. T. Suemoto, K. Tanaka, and A. Nakajima, J. Phys. Soc. Jpn. (Suppl. B) **63**, 190 (1994).
22. Y. Kanemitsu, S. Okamoto, M. Otobe, and S. Oda, Phys. Rev. B **55**, R7375 1996).
23. Y. Kanemitsu and S. Okamoto, Phys. Rev. B **58**, 9652 (1998).
24. D. Kovalev, H. Heckler, G. Polisski, and F. Koch, phys. stat. sol. (b) **215**, 871 (1999).
25. H. Kageshima, Surf. Sci. **357/358** (1996) 312.
26. N. F. Mott, Philos. Mag. B **43**, 941 (1981).
27. T. Tiedje, B. Abeles, and B. G. Brooks, Phys. Rev. Lett. **54**, 2545 (1985).
28. M. J. Estes and G. Moddel, Appl. Phys. Lett. **68**, 1814 (1996).
29. Y. Kanemitsu and Y. Fukunishi, in preparation.
30. Y. Kanemitsu and M. Iiboshi, in preparation.
31. Y. Takahashi, T. Furuta, Y. Ono, T. Ishiyama, and M. Tabe, Jpn. J. Appl. Phys. **34**, 950 (1995).
32. Y. Kanemitsu, and S. Okamoto, Phys. Rev. B **56,** R15561 (1997).
33. K. Nishimoto, D. Sotta, H. A. Durand, K. Etoh, and K. Ito, J. Lumin. **80**, 439 (1999).
34. S. Okamoto and Y. Kanemitsu, Solid State Commun. **103**, 573 (1997).
35. D. J. Lockwood, Z. H. Lu and J.-M. Baribeau, Phys. Rev. Lett. **76** (1996) 539.
36. S. B. Zhang and A. Zunger, Appl. Phys. Lett. **63**, 1399 (1993).
37. S. Miyazaki, K. Yamada, and M. Hirose, J. Non-Cryst. Solids **137/138**, 1119 (1991); S. Miyazaki and M. Hirose, Philos. Mag. B **60**, 23 (1989).
38. G. Allan, C. Delerue, and M. Lannoo, Mater. Res. Soc. Proc. **486**, 299 (1998).

(Received December 17, 1999; Accepted August 31, 2000)